Material response of metasurface integrated uncooled silicon germanium oxide SixGeyO1-x-y infrared microbolometers

Akshay Kumar Reddy Koppula, Amjed Abdullah, Tao Liu, Omar Alkorjia, Chen Zhu, et al.

Akshay Kumar Reddy Koppula, Amjed Abdullah, Tao Liu, Omar Alkorjia, Chen Zhu, Cameron Warder, Shayne Wadle, Phyllip Deloach, Savannah Lewis, Edward Kinzel, Mahmoud Almasri, "Material response of metasurface integrated uncooled silicon germanium oxide SixGeyO1-x-y infrared microbolometers," Proc. SPIE 11002, Infrared Technology and Applications XLV, 110021L (4 June 2019); doi: 10.1117/12.2519093

Event: SPIE Defense + Commercial Sensing, 2019, Baltimore, Maryland, United States

Material response of metasurface integrated uncooled silicon germanium oxide $Si_xGe_yO_{1-x-y}$ infrared microbolometers

Akshay Kumar Reddy Koppula[a], Amjed Abdullah[a], Tao Liu[b], Omar Alkorjia[a], Chen Zhu[c], Cameron Warder[a], Shayne Wadle[a], Phyllip Deloach[a], Savannah Lewis[a], Edward Kinzel[c], Mahmoud Almasri[a*]
[a] Department of Electrical and Computer Engineering, University of Missouri, Columbia, MO, USA; [b] Missouri University of Science and Technology, Department of Mechanical and Aerospace Engineering, 400 W. 13th St., Rolla, MO 65409 [c] University of Notre Dame, Department of Aerospace and Mechanical Engineering, Fitzpatrick Hall., Notre Dame, IN 46656

ABSTRACT

This paper presents a study of metasurface integrated microbolometers. The semiconductor absorber is sandwiched between a metal Frequency-Selective Surface (FSS) and ground plane. When the semiconductor absorber is electrically isolated from the ground plane by a thin dielectric it can be used to measure the temperature of the pixel. The integration with the FSS removes the need for a Fabry-Pérot cavity. The FSS allows control the attributes of radiation absorbed by the microbolometer on a pixel-by-pixel basis which provides the potential for spectral or polarimetric imaging. The FSS also affects he electrical performance of the semiconductor absorber and the thermal performance of the microbolometer. In addition, the complex permittivity of the semiconductor affects the optimal design of the FSS. The Si/Ge/O system is selected because it allows the properties of the absorber to be engineered (e.g., less oxygen gives lower absorptance and higher resistivity). This paper explores the absorber/FSS parameter space with an emphasis on the electrical and noise properties of the integrated system. Models are developed to explain results. Preliminary results show that the addition of the FSS improves TCR of the microbolometer by 10% while dramatically lowering its resistivity (factor of 5×). The resistivity reduction leads to a dramatic reduction of the noise power spectral density with the addition of FSS improving the measured 1/f noise by two orders of magnitude over an identical sample without the FSS. In addition, this paper will present the microbolometer figures of merits including voltage responsivity, detectivity, and thermal response time.
Keywords: Frequency-Selective Surface, Metasurface, Uncooled Microbolometer, SiGeO, TCR

1. INTRODUCTION

Microbolometers are uncooled infrared thermal sensors that shows a change in resistance in accordance with a change in temperature when they absorb IR radiation[1]. These devices find their eminent use in military, surveillance, law enforcement and security. Standard MEMS processing tools are used to fabricate the uncooled infrared microbolometer and we have integrated the Frequency selective surfaces into the device design. Microbolometers by their design are capable of absorbing Long Wave Infrared radiation (LWIR) ranging from 8-14 μm[2,3]. Frequency Selective Surfaces (FSS) are assemblies of antenna elements that provide an ensemble electromagnetic scattering response. They can be designed to impedance match the surface impedance to free-space leading to perfect absorption. Also called metasurfaces, they create a spectral response that is dependent on the sub-wavelength geometry as opposed to the material properties[5-8].

The most commonly used infrared sensitive materials are vanadium oxide (VO_x), amorphous silicon (α-Si), germanium silicon (GeSi) and yttrium barium copper oxide (YBaCuO)[3,4]. All these materials have a Temperature Coefficient of Resistance (TCR) ranging from 2-4%/K with a reasonably acceptable 1/f noise. The resistivity of most of these films go high with an increase in TCR which eventually increases their 1/f noise. This sometimes can be overcome with the help of doping but it can limit the TCR range. Silicon germanium oxide ($Si_xGe_yO_{1-x-y}$) on the other hand gives a good amount of TCR with acceptable range of resistivity and 1/f noise[9-12]. Different sensing materials and designs have been studied to approach a highrt absorption of the incident IR[13,14]. We have fabricated the amorphous $Si_xGe_yO_{1-x-y}$ in an RF magnetron sputtering system and integrated it as the infrared sensing layer in our uncooled infrared microbolometers. The electrical properties of all the fabricated films were first studied using a TCR testing setup and then the best composition was used as the IR sensing layer in the microbolometer. Various powers have been applied to individual Si and Ge 3” targets and the flow of oxygen determined activation energy, resistivity and TCR of these films.

Infrared Technology and Applications XLV, edited by Bjørn F. Andresen, Gabor F. Fulop, Charles M. Hanson, Proc. of SPIE Vol. 11002, 110021L
 · doi: 10.1117/12.2519093

Table 1. Parameters used in depositing the SiGeO films.

Substrates	Sputtering Targets	Output Power (W)	Temperature (^{0}C)	Pressure (Torr)	Thickness (nm)	Oxygen (SCCM)
Si	3" Si	50-320	Room Temperature	~3 x 10^{-6}	~300	0.002-1
Si_3N_4/SiO_2						
Glass	3" Ge	90-190				

The deposition time has been varied to keep the film thickness to be approximately 300nm. The base pressure in the sputtering chamber is almost less than $3x10^{-6}$ Torr all the times. Energy Dispersive X-ray spectroscopy (EDX) was used to study the atomic compositions of the fabricated $Si_xGe_yO_{1-x-y}$ films.

The Temperature Coefficient of Resistance (TCR) determines how drastically the resistance of a material reacts to the change in temperature. It is given by

$$TCR = \frac{1}{R}\frac{dR}{dT} = -\frac{E_a}{kT^2} \tag{1}$$

$$R(T) = R_0 \exp(\frac{E_a}{kT}) \tag{2}$$

where E_a is the activation energy, k is the Boltzmann constant, $R(T)$ is the resistance at temperature T, R_0 is an Arrhenius factor and is a constant. The value of E_a was calculated from the slope of Arrhenius plot.

The relationship between experimental resistance and the calculated resistivity of the deposited SiGeO films is given by

$$R = \int_s^{2s} \frac{\rho}{2\pi t}\frac{dx}{x} = \frac{\rho}{2\pi t}\, ln2 = \frac{V}{I} \tag{3}$$

$$\rho = \frac{\pi t}{ln2}\frac{V}{I} \tag{4}$$

where R is the resistance of the film, ρ is the sheet resistivity, t is the thickness of the thin film, s is the distance between any two adjacent probes on the 4-point, V and I are the measured voltage and current respectively.
The noise voltage Power Spectral Density (PSD) is defined by:

$$S_v = \frac{{V_n}^2}{\Delta f} \tag{5}$$

The microbolometer's performance is usually affected by the temperature fluctuation noise, background voltage noise and the sensitive element noise (Johnson noise and 1/f noise). Johnson noise given by ΔV_J is due to the thermal agitation of charge carriers.

$$\frac{\Delta V_J}{\sqrt{\Delta f}} = \sqrt{4k_BTR} \tag{6}$$

Where k_B is the Boltzmann constant, T is the room temperature in kelvin and R is the resistance of the microbolometer.

1/f noise, also called flicker noise, is a major limiting factor in the performance of a microbolometer design. This noise is usually generated at low frequencies and its magnitude is inversely proportional to the frequency. The 1/f noise can be expressed by Hooge's formula,

$$S_{\frac{1}{f}} = \frac{K_f(I_BR)^\beta}{f^\gamma} \tag{7}$$

2. FABRICATION OF UNCOOLED MICROBOLOMETER

The optimized design of the Frequency Selective Surface (FSS) integrated uncooled IR detector (pixel size as 40×40 μm^2) consists of a thin SiGeO IR sensitive layer sandwiched between the reflector and absorber of the resonator, creating a Metal-Insulator-Metal (MIM) configuration.

The fabrication of the microbolometer proceeds with the following steps: (a) thermal oxidation of the silicon wafer, deposition of chromium and gold trace layers, (b) curing and etching polyimide layers, (c) spin coating and patterning the sacrificial photoresist layer, deposition of silicon nitride layer and then lift off, (d) spin coating and patterning the sacrificial photoresist layer, deposition of aluminum and silicon oxide layer then lift off, (e) spin coating and patterning of sacrificial photoresist layer, depositing nickel chromium contacts followed by liftoff, (f) spin coating and patterning the sacrificial photoresist layer, deposition silicon germanium oxide and lift off, then spin coating and patterning the sacrificial photoresist layer, deposition aluminum layer for top layer of the metasurface and lift off, and then (g) ashing the polyimide. Figure (1) shows a cross sectional view of the fabricated layers.

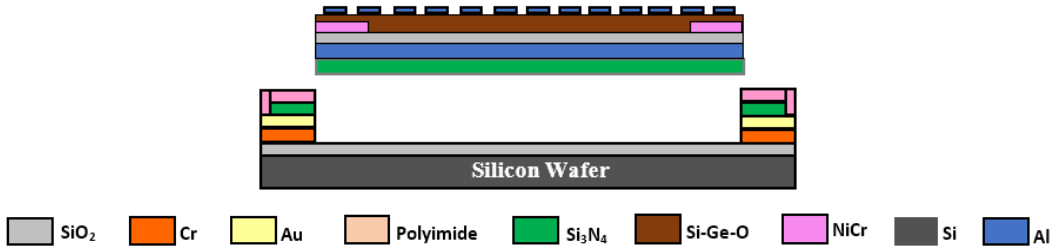

Figure)1(. Fabrication sideview of the uncooled infrared microbolometers.

3. RESULTS AND DISCUSSION

The temperature dependent resistance of the $Si_xGe_yO_{1-x-y}$ films are characterized using a 4-pont probe setup in a Janis VPF-100 cryostat. The resistance-temperature (R-T) and their relative temperature coefficient of resistance characteristics of these samples are studied using a programmable current source (Keithley Model 220) and a high precision voltmeter (Keithley model 2182 nano-voltmeter). Lakeshore 336 temperature controller is used to vary the temperature from 0°C to

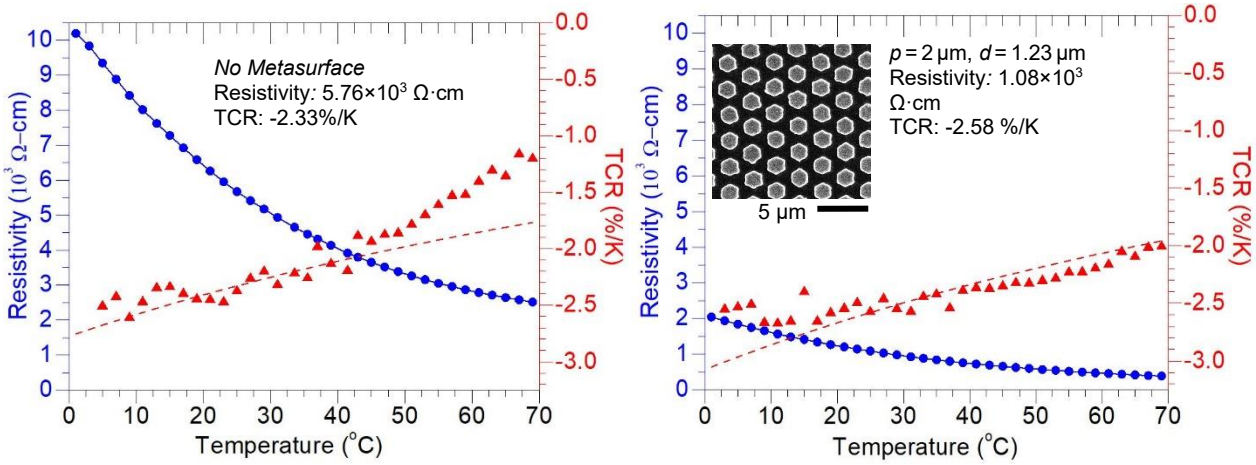

Figure)2(. Measured TCR and resistivity versus temperature for $Si_{0.655}Ge_{0.215}O_{0.130}$ without metasurface (a), and (b) with metasurface with center to center spacing, p, and discs diameter, d, of p = 2 µm, d = 1.23 µm. The resistivity was reduced by a factor of 5.3, while TCR was increased by 10%. The figure also shows SEMs micrographs of the patterned metasurface.

70°C with 2°C intervals. 150 data points were taken and averaged at each temperature set-point to study the R-T characteristics.

The results demonstrate the effects of including the metasurface, which slightly increases the TCR and dramatically reduces the resistivity. Depending on the stoichiometry, the TCR with metasurface increased while the resistivity is reduced by a greater extent (Figure 2). The preliminary results demonstrated that the addition of the metasurface with increasing discs fill factor have reduced the overall resistivity by a factor between 2.2 – 5.3, and increased TCR by 6% – 10%. The fill factor was increased by changing the center to center spacing (p) and diameter (d) of the discs (p=2 µm, d=0.92 µm; p=2µm, d=1.23 µm; p=3µm, d=1.30 µm). The resistivity and TCR for the film $Si_{0.655}Ge_{0.215}O_{0.130}$ demonstrated an overall improvement due to the composite structure (See Figure 2(b)). The figures show that the resistivity was reduced by a factor of 5.3 from 5.76×10^3 Ω-cm to 1.08×10^3 Ω-cm, while the TCR was increased by 10% from -2.33%/K to -2.58%/K.

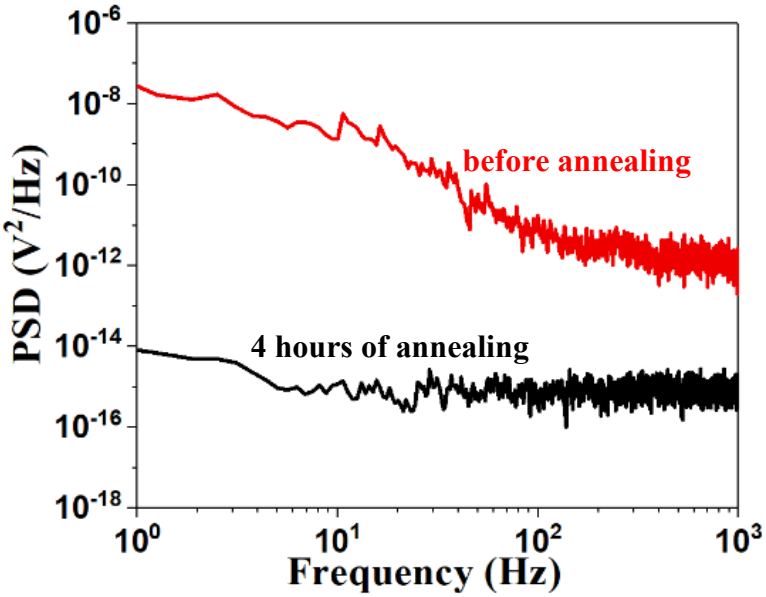

Figure (3). Noise power spectral density (PSD) of the microbolometer design before annealing and after 4 hours of vacuum annealing.

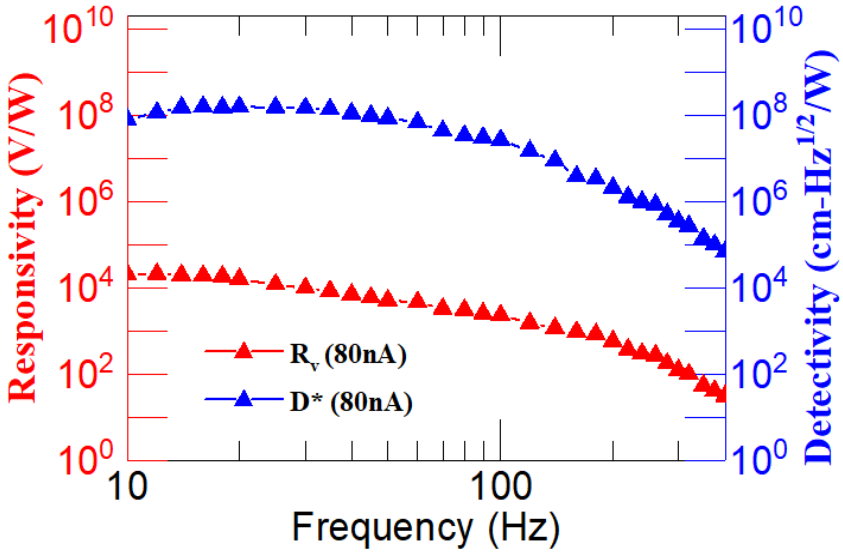

Figure (4). Measured voltage Responsivity and Detectivity as a function of chopper frequency at different current biases measured in vacuum with 2 to 13 µm broadband IR radiation.

Noise voltage PSD of the fabricated wafers were measured at atmospheric pressure inside a cryostat (DE 202 Cold head), placed inside an electromagnetic shielding room. Figure (3) shows the voltage noise PSD before and after annealing in vacuum at 300 °C for 4 hours using a bias current of 80 nA for microbolometer pixel size of 40×40 μm^2. The voltage noise PSD of the device decreases as the annealing time is increased. After 4 hours of annealing, the voltage noise started to increase. The lowest measured noise in vacuum annealing for the metasurface integrated microbolometer was 1.2×10^{-16} V^2/Hz. The corner frequency of the device, where Johnson noise meet $1/f$ noise was lowered to 10 Hz (from 200 Hz) after 4 hours annealing. In addition, the corresponding Hooge's parameters γ, β and K_f for the device were 1.02, 2.01, 2.637×10^{-14}, respectively.

The responsivity and detectivity were measured in vacuum at room temperature and plotted as a function of chopper frequency at different bias currents in Figure (4). The highest measured voltage responsivity and detectivity for the microbolometer with a pixel size of 40 μm × 40 μm^2 were 4.37×10^4 V/W and 1.19×10^9 cm-$Hz^{1/2}$/W respectively at a bias current of 80 nA. The responsivity and detectivity response were flat up to 100 Hz. The values obtained here for responsivity and detectivity are much larger than SiGeO, and amorphous Si microbolometers, and comparable to VO_x devices.

4. CONCLUSION

Frequency selective surface integrated uncooled infrared microbolometers are fabricated with the sensing layer integrated into the MIM layer. $Si_xGe_yO_{1-x-y}$ thin films are deposited by a simultaneous sputtering from two separate silicon and germanium targets in an RF magnetron sputtering system in the Ar/O_2 environment. The addition of metasurface with discs fill factor have reduced the resistivity by a factor between 2.2 – 5.3 and increased TCR by 6% - 10%. The highest measured voltage responsivity and detectivity for the microbolometer with a pixel size of 40 × 40 μm^2 were 4.37×10^4 V/W and 1.19×10^9 cm-$Hz^{1/2}$/W respectively. The lowest measured noise in vacuum annealing for the metasurface integrated microbolometer was 1.2×10^{-16} V^2/Hz.

ACKNOWLEDGEMENT

The project was supported by National Science Foundation, Grant Nos. 1509589 and 1653792. The first and second authors have equal weight.

REFRENCES

[1] Jalal, M., Hai, M. L., Ajmera, S., Almasri, M., "Noise Reduction of Amorphous SixGeyO1–x–yThin Films for Uncooled Microbolometers by Si3N4Passivation and Annealing in Vacuum," IEEE Sensors Journal 16(6), 1681–1691 (2016).

[2] Liu, T., Qu, C., Almasri, M., Kinzel, E., "Design and analysis of frequency-selective surface enabled microbolometers," Infrared Technology and Applications XLII (2016).

[3] Hai, M., Hesan, M., Lin, J., Cheng, Q., Jalal, M., Syllaios, J., Ajmera, S., Almasri, M., "Uncooled silicon germanium oxide ($Si_xGe_yO_{1-x-y}$) thin films for infrared detection," Infrared Technology and Applications XXXVIII, 835317 (2012).

[4] Cheng, Q., Almasri, M., "Silicon germanium oxide (Si x Ge 1-x O y) infrared material for uncooled infrared detection," Infrared Technology and Applications XXXV (2009).

[5] Cheng, Q., Almasri, M., "Characterization of radio frequency sputtered Si x Ge 1-x O y thin films for uncooled micro-bolometer," Infrared Technology and Applications XXXIV (2008).

[6] Qu, C., Kinzel, E. C., "Polycrystalline metasurface perfect absorbers fabricated using microsphere photolithography," Optics Letters 41(15), 3399 (2016).

[7] Tissot, J., Trouilleau, C., Fieque, B., Crastes, A., Legras, O., "Uncooled microbolometer detector: recent developments at ULIS," Opto-Electronics Review 14(1) (2006).

[8] Luukanen, A., Grossman, E., Miller, A., Helisto, P., Penttila, J., Sipola, H., Seppa, H., "An Ultra-Low Noise Superconducting Antenna-Coupled Microbolometer With a Room-Temperature Read-Out," IEEE Microwave and Wireless Components Letters 16(8), 464–466 (2006).

[9] Lucey, P. G., Horton, K. A., Williams, T., "Performance of a long-wave infrared hyperspectral imager using a Sagnac interferometer and an uncooled microbolometer array," Applied Optics 47(28) (2008).

[10] Ajmera, S. K., Syllaios, A. J., Tyber, G. S., Taylor, M. F., Hollingsworth, R. E., "Amorphous silicon thin-films for uncooled infrared microbolometer sensors," Infrared Technology and Applications XXXVI (2010).
[11] Schimert, T., Brady, J., Fagan, T., Taylor, M., Mccardel, W., Gooch, R., Ajmera, S., Hanson, C., Syllaios, A. J., "Amorphous silicon based large format uncooled FPA microbolometer technology," Infrared Technology and Applications XXXIV (2008).
[12] Murphy, D., Ray, M., Kennedy, A., Wyles, J., Hewitt, C., Wyles, R., Gordon, E., Sessler, T., Baur, S., et al., "Expanded applications for high performance VOx microbolometer FPAs," Infrared Technology and Applications XXXI (2005).
[13] Almasri, M., Butler, D., Celik-Butler, Z., "Self-supporting uncooled infrared microbolometers with low-thermal mass," Journal of Microelectromechanical Systems 10(3), 469–476 (2001).
[14] Norton, P. W., Kohin, M., Dovidio, M., Backer, B. S., "Commercialization of uncooled infrared technology," Infrared Systems and Photoelectronic Technology (2004).